Intracellular Concentration Gradients That Mirror External Gradients in Microfluidic Flows: A Computational Analysis

Varun Aggarwal & Tanmay P. Lele

Cellular and Molecular Bioengineering

ISSN 1865-5025

Cel. Mol. Bioeng.
DOI 10.1007/s12195-016-0474-3

Springer

Cellular and Molecular Bioengineering (© 2016)
DOI: 10.1007/s12195-016-0474-3

Intracellular Concentration Gradients That Mirror External Gradients in Microfluidic Flows: A Computational Analysis

VARUN AGGARWAL and TANMAY P. LELE

Department of Chemical Engineering, University of Florida, Gainesville, FL 32611, USA

(Received 12 September 2016; accepted 29 November 2016)

Associate Editor Michael R. King oversaw the review of this article.

Abstract—The generation of stable intracellular concentration gradients is a useful method for local control of cell function, selective manipulation of cellular structures and testing hypotheses related to dynamical intracellular processes. Cell culture in a microfluidic device allows the presentation of a stable gradient of small molecules across a single cell. This method has been used to selectively label mitochondria in portions of the cell, trypsinize specific cellular domains, and trigger receptor-mediated endocytosis in specific portions of the cell. Given the small length scales of a typical cell (~30 μm) and short cytoplasmic diffusive time scales of small molecules, it is surprising that cells can be labeled locally with this method. Here we developed models to explore the parametric space over which stable intracellular concentration gradients can be maintained in a microfluidic device. We show that gradients can develop and be maintained indefinitely for high rates of mass transfer across the membrane compared with diffusion, that is, for Sherwood number greater than 1. We show how these gradients can result in gradients in ligand–receptor binding and enzyme substrate binding. This analysis can help interpret and design microfluidic experiments for cytoplasmic partitioning.

Keywords—Mathematical model, Cytoplasmic partitioning, Convection, Diffusion, Receptor–ligand binding, Enzyme substrate reaction.

INTRODUCTION

The generation of spatially varying concentration of small molecules in the cytoplasmic space of living cells can allow the selective manipulation of cellular structures, control over cell function and the testing of hypotheses related to dynamical intracellular processes.[20] One approach pioneered by the Whitesides and Ingber groups is to culture single cells in microfluidic devices. By including small molecules in only one of two laminar streams that flow over the cell, it is possible to impose a step gradient in concentration of these molecules over a single cell. Whitesides and coworkers demonstrated the labeling of mitochondrial structures over specific spatial domains in the cell over long periods of time (minutes).[20] They similarly used this method to detach portions of the cell and to disrupt cytoskeletal structures over pre-chosen domains.[21]

Since then, microfluidics-based biological labeling has found use in a number of studies. Local damage of neuritis with a detergent was in a microfluidic device to study subsequent repair.[9] Another study treated cells locally with epidermal growth factor (EGF), and studied the spatial and temporal propagation of EGF signaling.[17] Multiple microfluidic streams have been used to apply a continuous gradient of growth factors (GF) to populations of neural stem cells in order to investigate the correlation of differentiation or proliferation with growth factor concentrations.[10] Confluent epithelial cells have been exposed to chemical gradients in microfluidic devices in order to selectively induce gene expression in a band of cells.[5] Temperature gradients have also been created in microfluidic devices to study patterning in drosophila[2] and multiples streams have been used for generating electricity from organic matter.[11]

As these studies show, there is a broad range of applications of microfluidic devices in treating cells with gradients of soluble factors. In this paper, we are interested in the development and maintenance of sub-cellular gradients. Previous studies Refs. 20,21 that sought to create intracellular gradients do not report measurement of the cytoplasmic gradient of the freely diffusing small molecules. This is likely due to the low cytoplasmic fluorescence compared with the localized fluorescence from sub-cellular organelles that bind (and therefore concentrate) small molecules. While it is reasonable to deduce from the spatially distributed labeling, or spatially selective action of small molecules

Address correspondence to Tanmay P. Lele, Department of Chemical Engineering, University of Florida, Gainesville, FL 32611, USA. Electronic mail: tlele@che.ufl.edu

Published online: 16 December 2016

(such as local cytoskeletal disruption) that the small molecule must partition spatially in the cytoplasmic space, it would appear challenging to maintain cytoplasmic gradients for significant lengths of time. Unlike the external gradients which are maintained because of laminar flow in the microfluidic device, there is no flow in the cell. Moreover, the length scales of cells are small (~30 μm), and diffusion coefficients in the cytoplasm of small molecules are large (~100 $\mu m^2/s$).[12]

Here we formulated models that account for mass transfer across the cell membrane, cytoplasmic diffusion through the cytoplasm, and reaction. We show that the intracellular gradient depends on the relative rates of mass transfer to diffusion. We predict the development of gradients in the cytoplasm of ligand-cytoplasm receptor binding and enzyme substrate binding. This model can provide guidance on the interpretation and design of microfluidic experiments for sub-cellular partitioning.

MODEL

Ligand Concentration When No Reaction

Because the length of the cell is much greater than the height, we modeled the concentration of the ligand in the cytoplasm with a one dimensional reaction diffusion equation (Eq. (1))

$$\frac{\partial C_L}{\partial t} = D_L \frac{\partial^2 C_L}{\partial x^2} + k_m[C_{L0}\mathrm{H}(l^* - x) - C_L] \quad C_L(x,0) = 0$$
$$\mathrm{H}(l^* - x) = 1,\ l^* \geq x = 0,\ l^* < x \tag{1}$$

Equation (1) describes the spatial and temporal variation in the cytoplasmic concentration of the ligand. Here C_L is the concentration of the ligand in the cytoplasm, D_L is the cytoplasmic diffusion coefficient of the ligand, k_m is the modified membrane mass transfer coefficient, l^* is the length of the treated part of the cell) over which there is flux of the ligand into the cell and C_{L0} is the concentration of the ligand in the external stream.

The length of the cell (l) was chosen as the length scale, concentration of the ligand in the external stream (C_{L0}) as the concentration scale, and the characteristic cytoplasmic diffusion time of the ligand ($t_L = \frac{l^2}{D_L}$) as the time scale for non-dimensionalizing Eq. (1). The non-dimensionalized equation is

$$\frac{\partial \theta_L}{\partial \tau} = \frac{\partial^2 \theta_L}{\partial \xi^2} + Sh[\mathrm{H}(\omega - \xi) - \theta_L] \qquad \theta_L(\xi,0) = 0 \tag{2}$$

here $\theta_L = \frac{C_L}{C_{L0}}$, $\tau = \frac{t}{t_L}$, $\xi = \frac{x}{l}$, $\omega = \frac{l^*}{l}$ and $Sh = \frac{k_m l^2}{D_L}$. Sh is the Sherwood number (based on the modified mass transfer coefficient) and it describes the relative rate of mass transfer across the cell membrane with respect to diffusion in the cytoplasm.

Receptor Ligand Binding

We extended the model developed in the previous section to reversible receptor–ligand binding in the cytoplasm. This model could apply (for example) to cytoplasmic hormone receptors, or membrane bound receptors like IP3, which is located on the ER membranes.

$$\frac{\partial C_L}{\partial t} = D_L \frac{\partial^2 C_L}{\partial x^2} + k_m[C_{L0}\mathrm{H}(l^* - x) - C_L] + k_{off}C_P - k_{on}C_R C_L \qquad C_L(x,0) = 0 \tag{3}$$

$$\frac{\partial C_R}{\partial t} = D_R \frac{\partial^2 C_R}{\partial x^2} + k_{off}C_P - k_{on}C_R C_L \qquad C_R(x,0) = C_{R0} \tag{4}$$

$$\frac{\partial C_P}{\partial t} = D_P \frac{\partial^2 C_P}{\partial x^2} - k_{off}C_P + k_{on}C_R C_L \qquad C_P(x,0) = 0 \tag{5}$$

Equations (3)–(5) describe the cytoplasmic concentration profiles of the ligand (C_L), receptor (C_R), and bound receptor (C_P) respectively. D_L,D_R, and D_P, and are their respective diffusion coefficients, k_{off} is the dissociation rate constant, and k_{on} is the binding rate constant. $K_d = \frac{k_{off}}{k_{on}}$ is the equilibrium dissociation constant for the reaction.

Choosing l as the length scale, cytoplasmic diffusion time of the receptor $t_R = \frac{l^2}{D_R}$ as the time scale, C_{L0} and C_{R0} as the concentration scales for ligand and receptor respectively, and assuming $D_P \approx D_R$ (for example, Ref. 7), Eqs. (3)–(5) were non-dimensionalized to:

$$\frac{\partial \theta_L}{\partial \tau} = a_L \frac{\partial^2 \theta_L}{\partial \xi^2} + a_L\, Sh\,[\mathrm{H}(\omega - \xi) - \theta_L] + Da_{off}\,\gamma\,\theta_P - Da_{on}\,\gamma\,\theta_L\,\theta_R \qquad \theta_L(\xi,0) = 0 \tag{6}$$

$$\frac{\partial \theta_R}{\partial \tau} = \frac{\partial^2 \theta_R}{\partial \xi^2} + Da_{off}\theta_P - Da_{on}\theta_L\theta_R \qquad \theta_R(\xi,0) = 1 \tag{7}$$

$$\frac{\partial \theta_P}{\partial \tau} = \frac{\partial^2 \theta_P}{\partial x^2} - Da_{off}\theta_P + Da_{on}\theta_L\theta_R \qquad \theta_P(\xi,0) = 0 \tag{8}$$

here $\theta_R = \frac{C_R}{C_{R0}}$, $\theta_P = \frac{C_P}{C_{R0}}$, $\tau = \frac{t}{t_R}$, $\gamma = \frac{C_{R0}}{C_{L0}}$, $a_L = \frac{D_L}{D_R}$, $Da_{on} = \frac{k_{on}C_{L0}l^2}{D_R}$ and $Da_{off} = \frac{k_{off}l^2}{D_R}$. The dimensionless equilibrium dissociation constant is $K_d' = \frac{K_d}{L_0}$. Da_{off} and Da_{on} are the Damkohler number for dissociation and binding. They describe the relative rate of dissociation and binding (respectively) with respect to the cytoplasmic diffusion rate of the receptor.

Membrane-Receptor Ligand Binding

A membrane embedded receptor is assumed to bind reversibly with the extracellular ligand to form a receptor ligand complex. The ligand is assumed to be membrane impermeable. This is different from before because there is no mass transfer across the cell membrane. The equations describing the spatially and temporally varying concentration of the free receptor (Eq. (9)) and the bound receptor (Eq. (10)) are below:

$$\frac{\partial C_R}{\partial t} = D_R\frac{\partial^2 C_R}{\partial x^2} - k_{on}\mathrm{H}(l^* - x)C_RC_{L0} + k_{off}C_P \qquad C_R(x,0) = C_{R0} \tag{9}$$

$$\frac{\partial C_P}{\partial t} = D_P\frac{\partial^2 C_P}{\partial x^2} + k_{on}\mathrm{H}(l^* - x)C_RC_{L0} - k_{off}C_P \qquad C_P(x,0) = 0 \tag{10}$$

In Eqs. (9) and (10), C_R is the membrane concentration of the receptor and C_P is the membrane concentration of the bound receptor. D_R and D_P are the membrane diffusion coefficients of the free receptor and the bound receptor respectively, k_{off} is the dissociation rate constant, k_{on} is the binding rate constant. $K_d = \frac{k_{off}}{k_{on}}$ is the equilibrium dissociation constant for the reaction.

Using the same scaling scheme defined in the receptor ligand binding section (the difference is that the parameters refer to properties of membrane-embedded receptors) and assuming that $D_P \approx D_R$. Eqs. (9) and (10) were non dimensionalized to:

$$\frac{\partial \theta_R}{\partial \tau} = \frac{\partial^2 \theta_R}{\partial \xi^2} - Da_{on}\,\mathrm{H}(\omega - \xi)\theta_R + Da_{off}\theta_P \qquad \theta_R(\xi,0) = 1 \tag{11}$$

$$\frac{\partial \theta_P}{\partial \tau} = \frac{\partial^2 \theta_P}{\partial \xi^2} + Da_{on}\,\mathrm{H}(\omega - \xi)\theta_R - Da_{off}\theta_P \qquad \theta_P(\xi,0) = 0 \tag{12}$$

The mathematical form of the parameter groups in Eqs. (11) and (12), is the same as the previous section. Da_{on} and Da_{off} under this situation describe the relative rate of binding and dissociation (respectively) to the membrane diffusion rate of the receptor.

Enzyme Substrate Binding

Substrate diffuses from the external stream across the membrane and is catalyzed by a cytoplasmic enzyme to a product. The product is assumed to be able to diffuse across the cell membrane. Equations (13) and (14) describe the cytoplasmic concentration profile of the substrate and the product respectively.

$$\frac{\partial C_S}{\partial t} = D_S\frac{\partial^2 C_S}{\partial x^2} - \frac{R_{max}C_S}{K_M + C_S} + k_m[\mathrm{H}(l^* - x)C_{S0} - C_S] \qquad C_S(x,0) = 0 \tag{13}$$

$$\frac{\partial C_P}{\partial t} = D_P\frac{\partial^2 C_P}{\partial x^2} + \frac{R_{max}C_S}{K_M + C_S} - k_{mp}C_P \qquad C_P(x,0) = 0 \tag{14}$$

here C_S and C_P are the cytoplasmic substrate and the cytoplasmic product concentration respectively, D_S and D_P are the cytoplasmic diffusion coefficients of the substrate and the product respectively, k_{ms} and k_{mp} are the modified cell-membrane mass transfer coefficients of the substrate and product respectively. The term $k_{mp}P$ refers to the efflux of product from the cell. K_M is the Michaelis–Menten constant, and R_{max} is the maximum rate. Choosing C_{S0} as the concentration scale, l as the length scale, $t_S = \frac{l^2}{D_S}$ as the time scale and assuming $D_S \approx D_P$ and $k_{mp} \approx k_m$, Eqs. (13) and (14) were non-dimensionalized to

$$\frac{\partial \theta_S}{\partial \tau} = \frac{\partial^2 \theta_S}{\partial \xi^2} - \frac{Da_M\theta_S}{\tilde{K}_M + \theta_S} + Sh[\mathrm{H}(\omega - \xi) - \theta_S] \qquad \theta_S(\xi,0) = 0 \tag{15}$$

$$\frac{\partial \theta_P}{\partial \tau} = \frac{\partial^2 \theta_P}{\partial \xi^2} + \frac{Da_M\theta_S}{\tilde{K}_M + \theta_S} - Sh\,\theta_P \qquad \theta_P(\xi,0) = 0 \tag{16}$$

In Eqs. (15) and (16) $\theta_S = \frac{C_S}{C_{S0}}$, $\theta_P = \frac{C_P}{C_{S0}}$, $Da_M = \frac{R_{max}l^2}{C_{S0}D_S}$, $\tilde{K}_M = \frac{K_M}{C_{S0}}$ and $Sh = \frac{k_m l^2}{D_S}$.

Finite Element Calculation

COMSOL 5.1 was used to solve the equations. Transport of dilute species (tds) module was used to

generate spatially and temporally dependent concentration profiles for different species. Steady state was verified by ensuring that the spatial concentration profiles overlapped completely for longer time instants.

RESULTS

External Gradients of Membrane-Permeable Ligands can Result in Intra-cellular Gradients

An elongated cell is assumed to be adherent to the bottom of a microfluidic device and oriented perpendicular to the direction of flow (Fig. 1a). Of the two streams flowing over the cell, only one contains the ligand. Negligible lateral mixing in the channel is assumed,[19] such that the external concentration profile across the cell can be assumed to be a step function. The ligand is modeled to enter the cell by transport through the cell membrane with a modified mass transfer coefficient k_m ($k_m = k/h$, here k is the mass transfer coefficient across the membrane, and h is the height of the cell) and then to diffuse within the cytoplasm with diffusion coefficient D_L. Here we assume that the cell is much thinner vertically than its length, which allows us to ignore gradients in the vertical direction.[21]

To understand the behavior of the ligand in the cytoplasm in the absence of any 'reaction', the one dimensional transport equation was solved at steady state under an external step gradient. 30% of the cell length was assumed to be treated with ligand-containing flow.[21] Shown in Fig. 1b is the predicted concentration profile for different values of *Sh* (the Sherwood number). *Sh* quantifies the relative time scale of transport across the membrane to the diffusion time scale across the length of the cell ($Sh = \frac{k_m l^2}{D_L}$, l is the length of the cell, see modeling section). For $Sh < 1$, transport across the membrane is slow compared to diffusion inside the cell, and the concentration profile in the cytoplasm is nearly uniform. For $Sh >> 1$, membrane transport becomes faster than intracellular diffusion, and the concentration profile approaches the step-function of the extracellular concentration profile. The rapid decay in the intracellular concentration at high *Sh* values is because of the high efflux rate across the untreated cell membrane relative to the rate of diffusion along the cell length. Significantly, such gradients can be maintained indefinitely; also it is possible to achieve $Sh > 1$ for biological ligands (Tables 1 and 2). Figure 1c shows the effect of the fractional treated length of the cell ($\omega = \frac{l^*}{l}$, l^* is the length of the treated part of the cell) on the concentration profile. The difference in intracellular concentration across the length of the cell is maximized when the interface is positioned at the mid-point of the cell.

Receptor Ligand Binding

We extended the model developed in the previous section to also account for cytoplasmic receptor–ligand binding. The ligand was assumed to diffuse across the membrane and bind reversibly to a receptor present in the cytoplasm. *Sh* was assumed to be greater than 1 to ensure a spatial gradient in the ligand concentration (see analysis above). The rate of binding relative to the rate of diffusion is expected to affect the gradients in bound receptor concentration. We therefore calculated bound receptor concentration profiles for different values of the Damkohler number Da_{on} ($Da_{on} = \frac{k_{on} C_{L0} l^2}{D_R}$, reflects the rate of binding relative to the rate of diffusion). We chose parameter values such that the receptor is not in large excess to the ligand (because then the ligand cannot impact receptor concentration) and the values were biologically reasonable (the range of parameters used here is consistent with experimentally measured parameters, see Tables 1 and 2). As seen in Fig. 2a, larger concentration differences in bound receptor concentration across the length of the cell are predicted for larger values of Da_{on} at steady state which reflect the larger spatially dependent net reaction rate (rate of binding − rate of dissociation, see Eq. (4)). Here, Da_{off} which is the Damkohler number for dissociation ($Da_{off} = \frac{k_{off} l^2}{D_R}$) is fixed at 100 ($Da_{off}$ is also an important parameter that determines the gradient, which we explore in Fig. 2b). For $Da_{on} = 1000$, that is for high Da_{off} and high Da_{on} the reaction is close to local equilibrium (Figure S2A, green curve) which determines the spatial gradient.

Figure 2b shows the effect of larger values of the Damkohler number based on the dissociation rate constant for fixed Da_{on}. Despite large Da_{on} (binding much faster than diffusion), no gradients are observed at steady state for $Da_{off} < 1$ (dissociation much slower than diffusion). Because the bound receptor preferentially diffuses rather than dissociates, most of the receptor is in a bound state regardless of the spatial position (the reaction is not at equilibrium as indicated by the plot of net relative rates, Figure S2B, $Da_{off} < 1$). Thus, for significant steady state gradients, both Da_{on} and Da_{off} have to be greater than 1. An example of this is mitochondrial labeling with red and green Mitotracker dye (Fig. 1C–D in Ref. 20). According to the analysis above $Da_{on} > 1$ (slow diffusivity/motion of mitochondria[3]) and $Da_{off} \approx 0$ (nearly irreversible binding of Mitotracker to mitochondria[15]). As Da_{off} is not greater than 1, the initial local labeling (Fig. 1C in

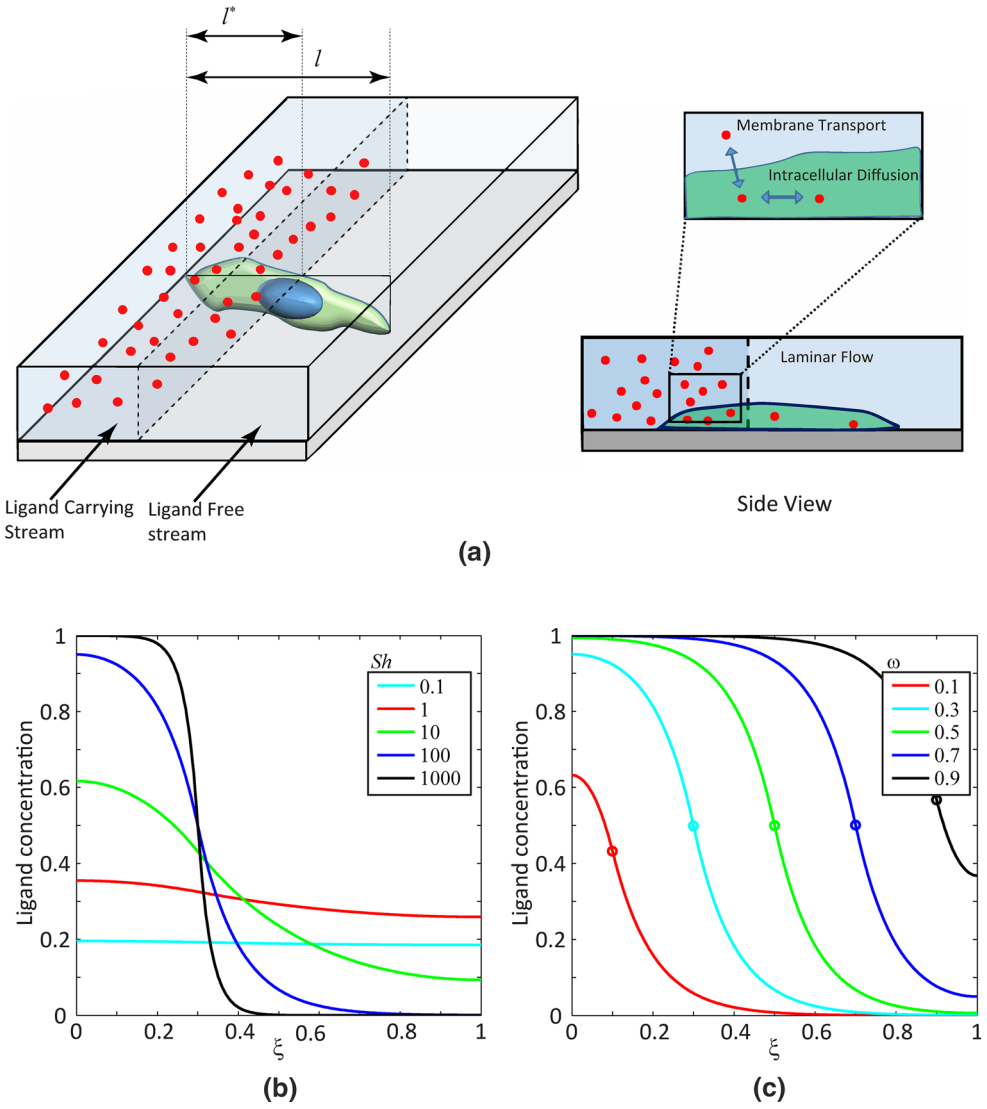

FIGURE 1. Cytoplasmic concentration of ligand under an external gradient. (a) Schematic of the experimental system. Ligand is present in one of the streams. Diffusional mixing between two streams is assumed to be negligible. (b) Cytoplasmic concentration of the ligand for different values of the Sherwood number ($\omega = 0.3$; this is the fractional treated length of the cell). A steeper gradient is observed for higher values of the Sherwood number. (c) Variation in the gradient for changing values of the treated cell length (ω is the fractional treated length of the cell, circles indicate the location of the interface). The difference in intracellular concentration across the length of the cell is maximum when $\omega = 0.5$. *Sh* = 100 for the calculations in (c).

Ref. 20) owing to fast binding compared to cytoplasmic diffusion is not observed to persist due to subsequent mixing over hours (Fig. 1D in Ref. 20). Also, $K_d^{'}$ ($K_d^{'} = \frac{Da_{off}}{Da_{on}}$) should be smaller than 1, as otherwise, there is little binding and very low levels of bound receptor in the cytoplasm (Figure S3, $K_d^{'} = 10$).

We performed the same analysis for membrane receptor ligand binding (see model section for the model equations). This scenario is different from the above case as the ligand is membrane-impermeable. We assume a step gradient in extracellular ligand as before. This implies that the membrane receptor can be bound only in the treated part of the cell membrane whereas the dissociation from the (diffusing) bound receptor can occur throughout the cell length. Figure 3 shows the concentration of the bound receptor and net reaction rates for different values of the Da_{on} and Da_{off}. As expected, both Da_{on} and Da_{off} have to be larger than one for spatial gradients to exist.

Enzyme Substrate Reaction

We next explored how extracellular substrate gradients could result in spatially distributed enzyme catalyzed reactivity and spatial gradients in the product of reaction at steady state. We considered a model

TABLE 1. Experimental values of parameters.

Name	Symbol used	Value or range	source
Length of the cell	l	~30 μm	Measured from images taken from Ref. 21
Treated length	l^*	~10 μm	Measured from images taken from Ref. 21
Diffusion coefficient of the ligand/substrate	D_L or D_S	~100 $\mu m^2\ s^{-1}$	For example, Ref. 12
Membrane mass transfer coefficient of the ligand/substrate	k_m	~10 s^{-1}	Estimated from Ref. 14
Diffusion coefficient of the receptor (cytoplasmic)	D_R	~10 $\mu m^2\ s^{-1}$	For example, Ref. 18
Diffusion coefficient of the receptor (membrane)	D_R	~1 $\mu m^2\ s^{-1}$	For example, Ref. 8
Binding rate constant	k_{on}	~10^4–10^7 $M^{-1}s^{-1}$	For example, Refs. 6,1
Dissociation rate constant	k_{off}	~1–10^{-3} s^{-1}	For example, Refs. 6,16
Initial receptor concentration	C_{R0}	~1 μM	Estimated from Ref. 24
Ligand/substrate concentration in the external stream	C_{L0}, C_{S0}	~1 μM	Ref. 21
Max enzyme rate	R_{max}	0.01–10 $\mu M\ s^{-1}$	See for example, Ref. 23
Michaelis–Menten parameter	K_M	~1–100 μM	For example, Ref. 23

TABLE 2. Values of dimensionless parameter groups.

Name	Symbol used	Expression	Range
Ratio of diffusion coefficients	a_L	$a_L = \frac{D_L}{D_R}$	10
Fractional treated length of the cell	ω	$\omega = \frac{l^*}{l}$	0.3
Sherwood number	Sh	$Sh = \frac{k_m l^2}{D_L}$	100
Damkohler number for binding	Da_{on}	$Da_{on} = \frac{k_{on} C_{L0} l^2}{D_R}$	1–1000
Damkohler number for dissociation	Da_{off}	$Da_{on} = \frac{k_{off} l^2}{D_R}$	0.1–100
Damkohler number for binding (membrane)	Da_{on}	$Da_{on} = \frac{k_{on} C_{L0} l^2}{D_R}$	10–10,000
Damkohler number for dissociation (membrane)	Da_{off}	$Da_{on} = \frac{k_{off} l^2}{D_R}$	1–1000
Dimensionless equilibrium dissociation constant	$K_d^{'}$	$K_d^{'} = \frac{Da_{off}}{Da_{on}}$	0.01–10
Concentration ratio	γ	$\gamma = \frac{C_{R0}}{C_{L0}}$	1
Damkohler number for the enzyme reaction	Da_M	$Da_M = \frac{R_{max} l^2}{C_{L0} D_S}$	1–100
Non dimensionalized Michaelis–Menten constant	$\tilde{K}_M$	$\tilde{K}_M = \frac{K_M}{C_{S0}}$	1–100

The parameters in Table 1 were used to estimate the values of dimensionless parameter groups in Table 2.

in which substrate is present in one stream, crosses the membrane into the cytoplasm, and is converted into product by an enzyme (see modeling section for details). The product is assumed to cross the membrane and leave. An example of such a type of reaction is glycogenolysis performed by liver cells.[13,22]

Two parameter groups determine the steady state substrate concentration in the cytoplasm—the Damkohler number Da_M based on the maximum reaction rate ($Da_M = \frac{R_{max} l^2}{C_{S0} D_S}$, here C_{S0} is the concentration of the substrate in the external stream, R_{max} is the maximum rate, and D_S is the cytoplasmic diffusion coefficient of the substrate, and l is the length of the cell, see model) and the Sherwood number Sh for transport of substrate across the membrane. Figure 4a shows the concentration profile of the substrate for different values of the Damkohler number and Sherwood number. For $Sh = 10$, the substrate concentration is spatially dependent because of fast mass transfer across the membrane compared to cytoplasmic diffusion. The parameter group Sh/Da_M determines the nature of the spatial gradient here. For $\frac{Sh}{Da_M} > 1$, where mass transfer dominates reaction, the substrate concentration is insensitive to reaction and little product is formed (Figs. 4a and 4b). For low Sh/Da_M, the product concentration and hence the spatial gradient is larger.

DISCUSSION

The creation of intracellular gradients by applying an extracellular step gradient in ligand concentration using a microfluidic device has been demonstrated in the past.[20,21] This method has been used to label intracellular organelles, detach selected portions of the cell, and cause spatially localized receptor internalization. Existence of cytoplasmic ligand gradients has been primarily inferred from selective binding of fluorescent ligand molecules to membrane-embedded receptors (e.g. in mitochondria,[20]). However, due to low fluorescence of diffuse ligand in the cytoplasm compared to bound organelles, cytoplasmic concen-

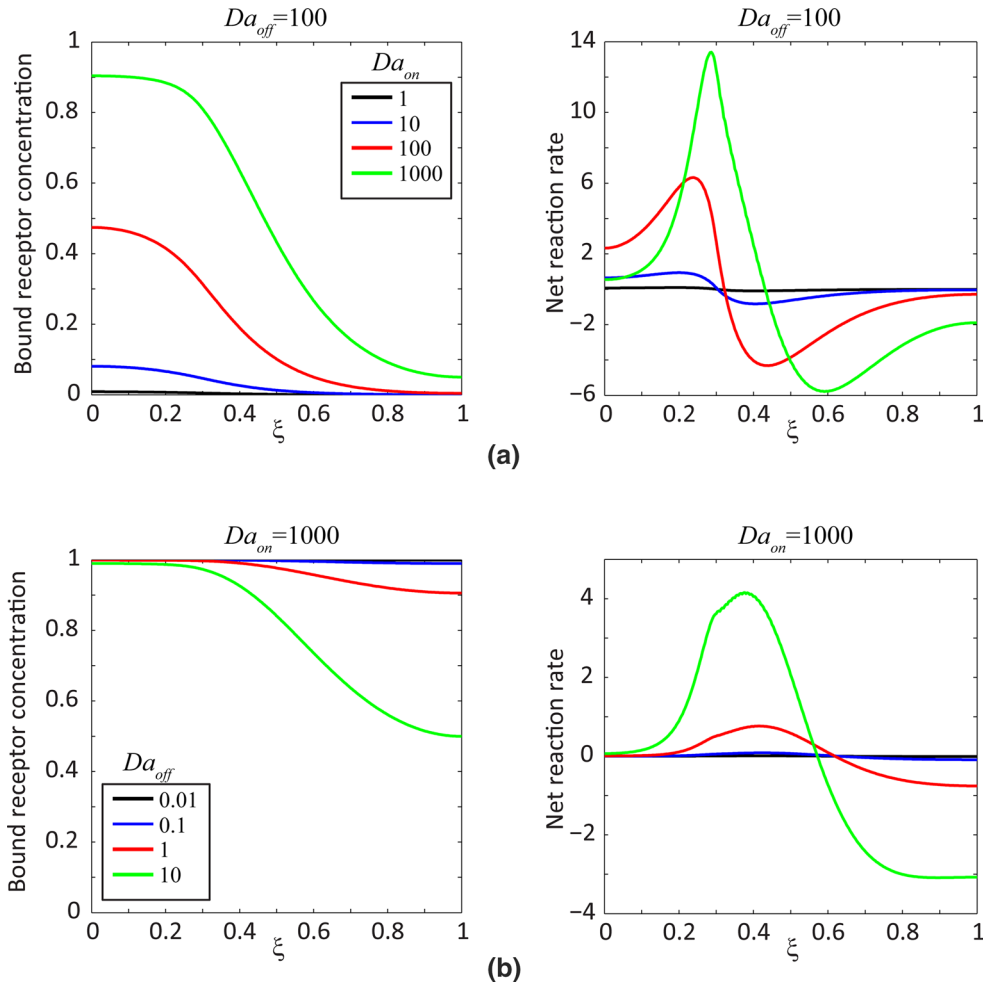

FIGURE 2. Effect of external ligand gradient on cytoplasmic receptor ligand binding. (a) Left: Concentration profile of the bound receptor at steady state for different values of Da_{on} ($Da_{off} = 100$). Differences in the concentrations are smaller for smaller values of Da_{on}. Right: Corresponding net reaction rate $Da_{on}\theta_R\theta_L - Da_{off}\theta_P$ (here θ_L, θ_R and θ_P are non dimensionalized concentration of the ligand, free receptor and bound receptor respectively); The net reaction rate is higher for high values of Da_{on}. (b) Left: Concentration profile of the bound receptor at steady state for different values of Da_{off}($Da_{on} = 1000$). No gradients are observed when Da_{off}<1. Right: Corresponding net reaction rate.

tration gradients of free ligand need to be inferred from observations of spatially local phenomena, such as binding or cell detachment.

To address this, Takayama et al. analyzed a mathematical model in which concentration of the small molecule was fixed at an intracellular plane of a one-dimensional cell, and solved a spatially-dependent partial differential equation for cytoplasmic concentration.[21] This model accounted for mass transfer across the membrane and cytoplasmic diffusion, but it made the unphysical assumption that there will be a constant concentration in the treated portion of the cell. We did not make this assumption but rather modeled the entire cell (i.e. the portion in the treated stream as well). A novel aspect of this work is that we identified the Sherwood number as the pertinent parameter which governs the existence of intracellular ligand gradients (refer to Tables 1 and 2 for the value of the parameters and the definition of the non-dimensional groups, and to Tables 3 and 4 for the symbols used).

The model by Takayama et al. did not account for reaction in the cytoplasm. Yet, the purpose of creating ligand gradients is to cause local binding in the cytoplasm. Such reactions can (for example) be used to disrupt cytoskeletal structures locally (for example, Refs. 4,21) In this paper, we computationally investigated the development of gradients in receptor concentrations in response to extracellular step gradients in a microfluidic device. Our results demonstrate that steady-state receptor binding gradients can be established with the microfluidic technique, provided $Sh > 1$, and $Da > 1$. We showed that the Damkohler number (both based on binding rate and dissociation rate), is a second parameter that affects gradients in receptor

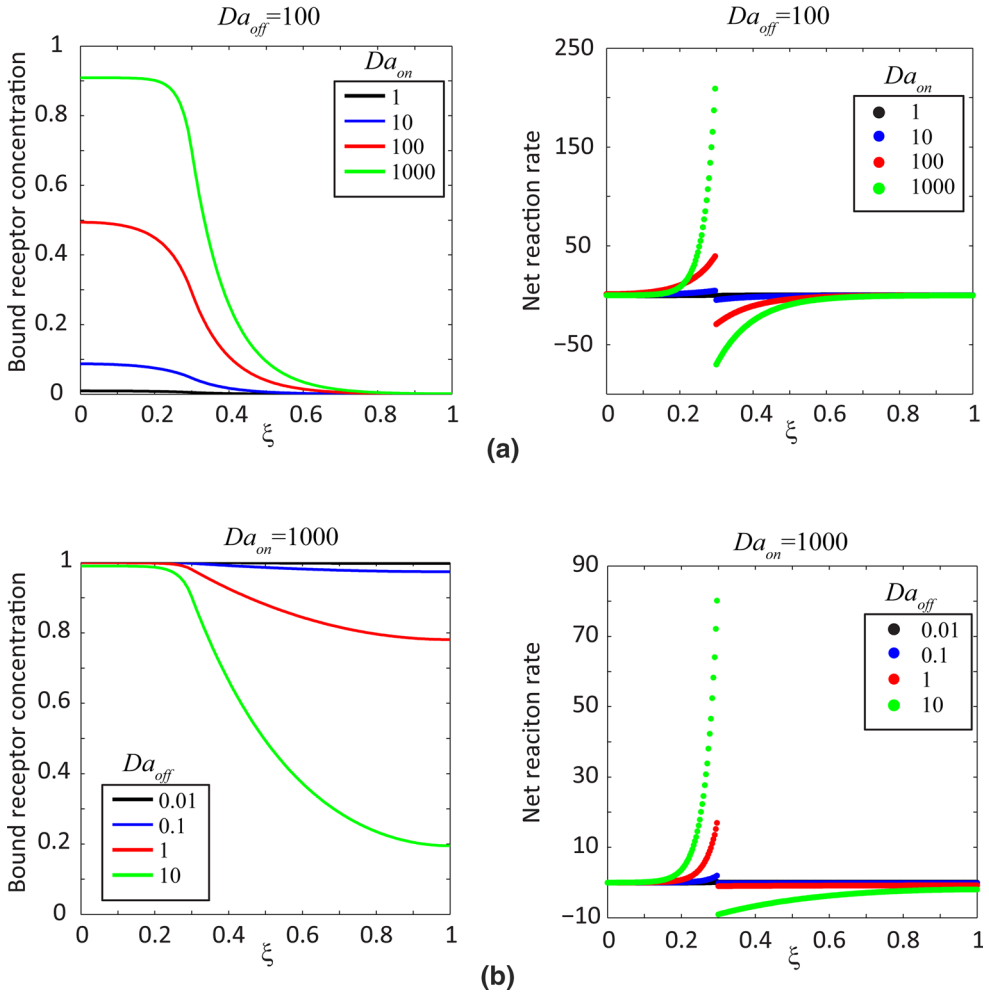

FIGURE 3. Effect of external ligand gradient on membrane receptor ligand binding. (a) Left: Concentration profile of the bound receptor at steady state for different values of Da_{on} $Da_{off} = 100$). Right: Corresponding net reaction rate, bound receptor is formed only in the treated part of the cell. (b) Left: Concentration profile of the bound receptor at steady state for different values of Da_{off}($Da_{on} = 1000$). Right: Corresponding net reaction rate.

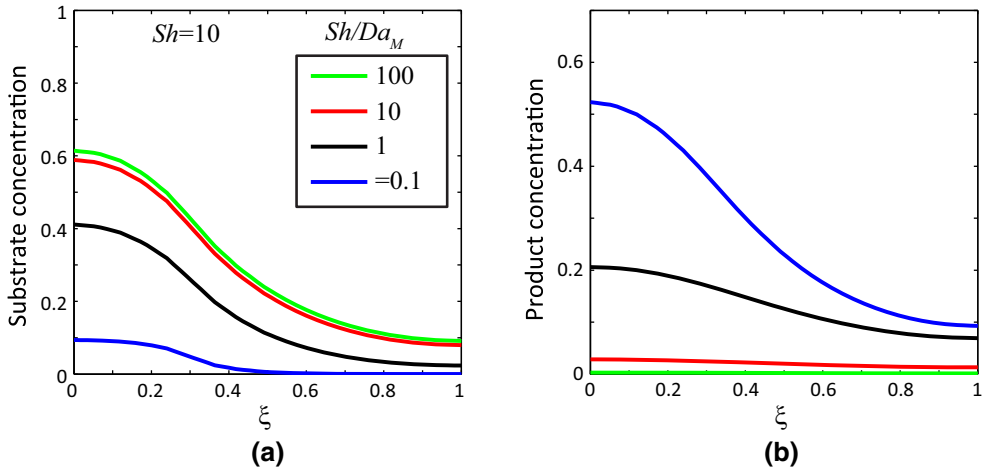

FIGURE 4. Effect of an external substrate gradient on cytoplasmic enzyme substrate reaction. (a) Cytoplasmic concentration of the substrate for different values of $\frac{Sh}{Da_M}$; $Sh = 10$. The reaction affects substrate concentration only when $\frac{Sh}{Da_M} \leq 1$ (compare with Fig. 1b). (b) Cytoplasmic concentrations of the product corresponding to the curves in (a).

TABLE 3. Symbols used.

Variables	Symbol used
Concentration of the ligand	C_L
Concentration of the receptor	C_R
Concentration of the bound receptor/enzyme-substrate reactivity product	C_P
Concentration of the substrate	C_S
Time	t
Space	x

TABLE 4. Symbols used for dimensionless variables.

Dimensionless variables	Symbol used
Concentration of the ligand	θ_L
Concentration of the receptor	θ_R
Concentration of the bound receptor/enzyme-substrate reactivity product	θ_P
Concentration of the substrate	θ_S
Time	τ
Space	ξ

concentration. We also show that it is possible to create steady-state gradients in enzyme-catalyzed reactivity and product concentration. The values of Sh, Da_{on}, Da_{off} or Da_M under which gradients develop are reasonable for biological applications (see Tables 1 and 2) based on measured parameters (Table 1). We hope that this work will provide new impetus to the use of microfluidic devices for sub-cellular spatial patterning and the spatial probing of sub-cellular processes.

ELECTRONIC SUPPLEMENTARY MATERIAL

The online version of this article (doi: 10.1007/s12195-016-0474-3) contains supplementary material, which is available to authorized users.

ACKNOWLEDGMENT

The authors gratefully acknowledge V.J. Tocco for helping during the initial edits of the paper and in making figure describing the schematic of the experiment, and Dr. Richard B. Dickinson for providing valuable insight and help in organizing the manuscript. This work was supported by the National Institutes of Health (www.nih.org) under Awards R01GM102486 (T.P.L.) and R01EB014869 (T.P.L.). The funders had no role in study design, data collection and analysis, decision to publish, or preparation of the manuscript.

CONFLICT OF INTEREST

Aggarwal V., and Lele T. P. both declare no conflict of interest.

ETHICAL STANDARD

No human or animal studies were carried out by the authors for this article.

REFERENCES

[1]Bajzer, Z., A. C. Myers, and S. Vuk-Pavlović. Binding, internalization, and intracellular processing of proteins interacting with recycling receptors. A kinetic analysis. *J. Biol. Chem.* 264:13623–13631, 1989.

[2]Benedetto, A., G. Accetta, Y. Fujita, and G. Charras. Spatiotemporal control of gene expression using microfluidics. *Lab Chip* 14:1336–1347, 2014.

[3]Bomzon, Z., M. M. Knight, D. L. Bader, and E. Kimmel. Mitochondrial dynamics in chondrocytes and their connection to the mechanical properties of the cytoplasm. *J Biomech Eng* 128:674–679, 2006.

[4]Burakov, A., E. Nadezhdina, B. Slepchenko, and V. Rodionov. Centrosome positioning in interphase cells. *J. Cell Biol.* 162:963–969, 2003.

[5]Chung, B. G., L. A. Flanagan, S. W. Rhee, P. H. Schwartz, A. P. Lee, E. S. Monuki, and N. L. Jeon. Human neural stem cell growth and differentiation in a gradient-generating microfluidic device. *Lab Chip* 5:401–406, 2005.

[6]Ciechanover, A., A. L. Schwartz, and H. F. Lodish. The asialoglycoprotein receptor internalizes and recycles independently of the transferrin and insulin receptors. *Cell* 32:267–275, 1983.

[7]Enns, C. A., and H. H. Sussman. Physical characterization of the transferrin receptor in human placentae. *J. Biol. Chem.* 256:9820–9823, 1981.

[8]Knight, J. D., M. G. Lerner, J. G. Marcano-Velázquez, R. W. Pastor, and J. J. Falke. Single molecule diffusion of membrane-bound proteins: window into lipid contacts and bilayer dynamics. *Biophys. J.* 99:2879–2887, 2010.

[9]Lee, C. Y., E. V. Romanova, and J. V. Sweedler. Laminar stream of detergents for subcellular neurite damage in a microfluidic device: a simple tool for the study of neuroregeneration. *J. Neural Eng.* 10:036020, 2013.

[10]Li, Z., Y. Zhang, P. R. LeDuc, and K. B. Gregory. Microbial electricity generation via microfluidic flow control. *Biotechnol. Bioeng.* 108:2061–2069, 2011.

[11]Lucchetta, E. M., J. H. Lee, L. A. Fu, N. H. Patel, and R. F. Ismagilov. Dynamics of *Drosophila* embryonic patterning network perturbed in space and time using microfluidics. *Nature* 434:1134–1138, 2005.

[12]Mastro, A. M., M. A. Babich, W. D. Taylor, and A. D. Keith. Diffusion of a small molecule in the cytoplasm of mammalian cells. *Proc. Natl. Acad. Sci. USA* 81:3414–3418, 1984.

[13]Nordlie, R. C., J. D. Foster, and A. J. Lange. Regulation of glucose production by the liver. *Annu. Rev. Nutr.* 19:379–406, 1999.

[14]Olofsson, J., H. Bridle, A. Jesorka, I. Isaksson, S. Weber, and O. Orwar. Direct access and control of the intracellular

solution environment in single cells. *Anal. Chem.* 81:1810–1818, 2009.
[15]Poot, M., Y. Z. Zhang, J. A. Kramer, K. S. Wells, L. J. Jones, D. K. Hanzel, A. G. Lugade, V. L. Singer, and R. P. Haugland. Analysis of mitochondrial morphology and function with novel fixable fluorescent stains. *J Histochem Cytochem* 44:1363–1372, 1996.
[16]Pruzansky, J. J., and R. Patterson. Limiting concentrations of human basophil-bound IgE antibody required for histamine release. *Immunology* 64:307–310, 1988.
[17]Sawano, A., S. Takayama, M. Matsuda, and A. Miyawaki. Lateral propagation of EGF signaling after local stimulation is dependent on receptor density. *Dev. Cell* 3:245–257, 2002.
[18]Skinner, A. L., and J. S. Laurence. High-field solution NMR spectroscopy as a tool for assessing protein interactions with small molecule ligands. *J. Pharm. Sci.* 97:4670–4695, 2008.
[19]Stroock, A., S. Dertinger, A. Ajdari, I. Mezic, H. Stone, and G. Whitesides. Chaotic mixer for microchannels. *Science* 295:647–651, 2002.
[20]Takayama, S., E. Ostuni, P. LeDuc, K. Naruse, D. Ingber, and G. Whitesides. Laminar flows—Subcellular positioning of small molecules. *Nature* 411:1016–1016, 2001.
[21]Takayama, S., E. Ostuni, P. LeDuc, K. Naruse, D. E. Ingber, and G. M. Whitesides. Selective chemical treatment of cellular microdomains using multiple laminar streams. *Chem. Biol.* 10:123–130, 2003.
[22]van Schaftingen, E., and I. Gerin. The glucose-6-phosphatase system. *Biochem. J.* 362:513–532, 2002.
[23]Viola, R. E. Kinetic studies of the reactions catalyzed by glucose-6-phosphate dehydrogenase from Leuconostoc mesenteroides: pH variation of kinetic parameters. *Arch. Biochem. Biophys.* 228:415–424, 1984.
[24]Waters, C. M., K. C. Oberg, G. Carpenter, and K. A. Overholser. Rate constants for binding, dissociation, and internalization of EGF: effect of receptor occupancy and ligand concentration. *Biochemistry* 29:3563–3569, 1990.